



Effect of sulfides addition in synthetic seawater solution on the corrosion of copper and its inhibition using the chitosan polymer

Khadija EL Mouaden^{1*}, Lahcen Bazzi¹

¹ Materials and Environment Laboratory, Department of Chemistry, Faculty of Sciences, Ibn Zohr University, Agadir, Morocco

Received 20 Jun 2016,
Revised 17 Oct 2016,
Accepted 23 Oct 2016

Keyword

- ✓ Pollution by sulfides,
- ✓ Cyclic voltammograms,
- ✓ Corrosion,
- ✓ Copper,
- ✓ Synthetic seawater.

khadija.elmouaden@gmail.com
+212 615881269

Abstract

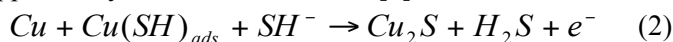
The electrochemical behavior of copper immersed in synthetic seawater (EMS) polluted by sulfide ions using Na₂S, 9H₂O was investigated by the corrosion potential, cyclic voltammetry measurements (CV), potentiodynamic polarization (PP) and electrochemical impedance spectroscopy (EIS). The corrosion studies are realized in synthetic seawater polluted by the sulfides at different concentrations in presence and absence of chitosan polymer chosen as tested inhibitor. The evolution of the open circuit potential of copper immersed in polluted seawater shows that E_{corr} decreases towards more negative values after addition of S²⁻. The CVs obtained indicate that the sulfide ions increase the current density of the oxidation peak of copper. The polarization curves and Nyquist diagrams mentioned that the sulfides addition provokes a diffusion palier in the anodic curve, so, the oxygen oxidation reaction was controlled by a diffusion mechanism in the presence of sulfides. However, the addition of different concentration of chitosan reduces the oxidation of copper in the presence of sulfides, which can suggest that chitosan protects the copper surface against the polluted and aggressive marine environment.

1. Introduction

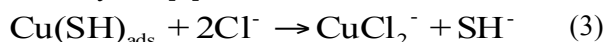
In most marine activities and processes, the corrosion rate of metals is accelerated with the presence of sulfur compounds such as S₂O₃²⁻, SO₃²⁻, S₂O₄²⁻, HS⁻ and H₂S species [1, 2]. But hydrogen sulfide (H₂S) is an extremely toxic element which increases the corrosion rate and accelerates the copper structure deterioration. The copper is chosen in this work, according to its thermodynamic stability and considerable resistance to corrosion in the marine environments. The most corrosive agent in the seawater is that the containers can be exposed to sulfide, issue from either mineral dissolution (like pyrite or FeS₂) or microbial production from sulfates (by the reaction of sulfate-reducing bacteria) [3-5]. Many studies have anticipated that Cu corrosion starts with the adsorption of the anion [6] in aqueous SH⁻ solutions [7]:



This reaction is followed by a second slow reaction using Cu to produce the Cu₂S as a film on the surface, in parallel this process was supported by H⁺ or H₂O reduction [7],



In the conditions of long-term tests, the Cu₂S film was formed at the copper surface. While Cu₂S was formed at a constant rate, the film can be considered partially protective, and corrosion can also be simplified by the complexation and solubilisation of Cu I by Cl⁻ [8]:



Since the solubility product of Cu I in SH⁻ solution is very small [7], any dissolved Cu I would be expected to eventually precipitate as Cu₂S:



When soluble sulfides are present in seawater, a thick black, feebly adherent scale forms on copper surface [6]. This scale is composed mainly by Cu₂S although CuS, Cu₂O and non-stoichiometric copper sulfide species such as Cu_{1.8}S have in addition been reported [9]. The sulfide pollution of seawater can be issue from industrial waste

discharge, biological and bacteriological reactions in seawater, which activate the corrosion of coppers. The solution contains the suspended particles such as waste particles and aggressive ions similar to chloride and sulfide which can have a considerable effect on the corrosion process of copper. The interaction of the suspended particles and aggressive ions with the copper interface in solution can result in corrosion reactions [10]. In this work, we desire to discover new lights about the corrosion of copper immersed in Na_2S containing sulfide ions using electrochemical measurements. To prevent the corrosion of copper, the use of polymer coatings is nowadays the most widespread approach yielding to the formation of an effective barrier against corrosive species contained in different environments. In the present work, we tested the effect of chitosan polymer on the corrosion of copper in seawater containing sulfides.

2. Experimental detail

2.1. Materials and chemicals

The material used for all experiments was prepared using copper 99.99% (weight percent), which was cut from a rectangular copper rod, with a total area of 0.20 cm^2 for the electrochemical tests. Before the electrochemical measurements, the specimens were polished successively with 600, 800, 1000, 1200 grade using sand papers. Then, the electrode was cleaned by washing with distilled water, acetone, distilled water, respectively, and immersed into the test solution. The electrolyte solution adopted in this study was artificial seawater prepared with the following composition (ASTM D 1141-90(1992): NaCl (24,53g), KCl (0,695g), MgCl_2 (5,20g), Na_2SO_4 (4,09g), CaCl_2 (1,16g) and NaHCO_3 (0,201g). The pH of the seawater was adjusted at 8.2 using 5 M NaOH solution. We are testing different concentration of sulfide containing solutions (Na_2S , $9\text{H}_2\text{O}$).

2.2. General aspects of chitosan

The chitosan polymer is a non-poisonous, biodegradable and functional biopolymer consisting primarily of β linked 2-amino-2-deoxy- β -D-glucopyranose units (Figure 1). It is used for diverse applications, like substrates for treatment and enzyme immobilization [11], separation membranes [12], and metal adsorbants for the removal of Hg(II) [13, 14], Cu(II) [15-18], Cr(III and VI) [19-21], Ag(I) [22], Fe(III) [23, 24], Mo(VI) [25] and Cd(II) [26] from ground and waste water. The chitosan is also used as bacterial inhibitor in different medium due to its bactericide properties [27]. We are interesting by testing the chitosan polymer effect on the copper corrosion in seawater + Na_2S , $9\text{H}_2\text{O}$.

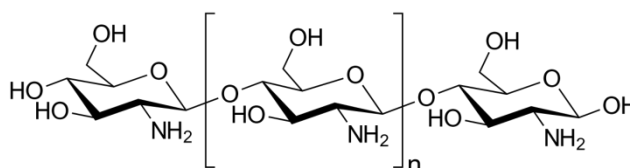


Figure 1: the molecular structure of chitosan

2.3. Electrochemical experiments

A conventional three electrode cell was used for all the electrochemical measurements. A saturated calomel electrode (SCE) was used as a reference electrode; a platinum electrode acts as a counter electrode and the copper is the working electrode. Synthetic seawater at different concentration of sulfide ions, served as the electrolyte. The behavior of copper and different reactions happening at the interface copper/solution are evaluated using the Open circuit potential (OCP), cyclic voltammetry (CV), electrochemical impedance and polarisation measurements by Voltalab PGZ 301 electrochemical analyzer under computer control. The OCP tests are investigated in order to control the potential of copper in synthetic seawater under immersion conditions for 30min with addition of sulfide ions at 10min. The CV was carried out for copper electrode in the artificial seawater solution + sulfide + chitosan. The working electrode is scanned from negative to positive values in the potential range of -600 mV to 400 mV at different scan rate. All measurements were taken at $25 \text{ }^\circ\text{C}$. The polarization curves were obtained by changing the electrode potential automatically from a cathodic potential of -600mV to an anodic one of 600mV vs SCE with a scan rate of 1 mV/s^{-1} . In other hand, the electrochemical impedance microscopy was carried out using AC signals of amplitude 10mV peak to peak at the open circuit potential in the frequency range of 100 KHz to 10 mHz .

2.4. Scanning electron microscopy (SEM)

The copper samples surface studied are exposed to synthetic seawater polluted by different concentration of sulfides for three months, and examined by a JEOL JSM-6480 LV scanning electron microscopy (SEM). This test can identify the attack effect of sulfides on the copper surface.

3. Results and discussion

3.1. The variation of corrosion potential

Figure 2 shows the evolution of the corrosion potential E_{corr} of copper during 30min in non-polluted and in polluted synthetic seawater by different concentration of sulfides.

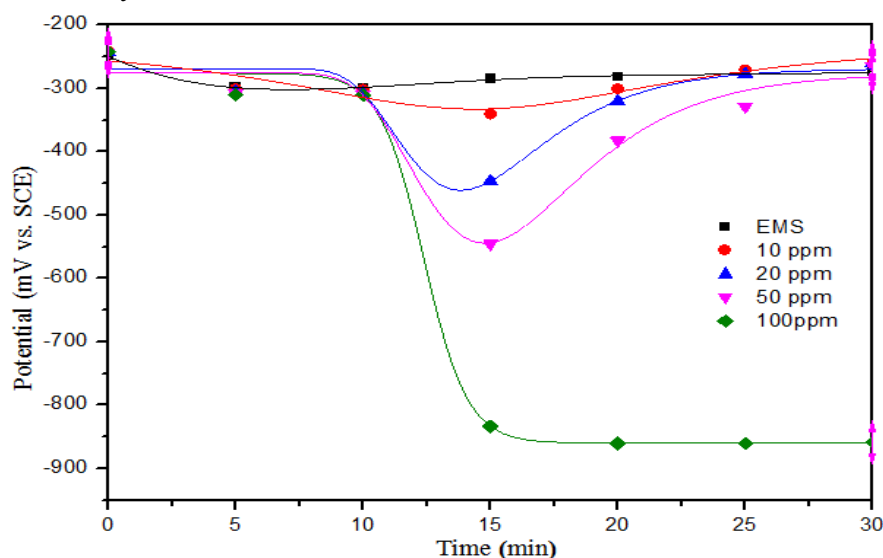


Figure 2: Open circuit potential for the copper immersed in synthetic seawater at different concentration of sulfide ions.

In the non-polluted environment, we observe that E_{corr} moves slightly towards a cathodic values when the time immersion increases. This phenomenon is probably due to the absence of oxygen in the solution which contributes to the destabilization of the passive sheet in a well-ventilated environment. The same phenomenon is observed in polluted seawater by the sulfide ions at a low concentration (1-10ppm). However, at high concentration (20, 50 and 100 ppm), it's remarkable that E_{corr} decreases towards a more negative values after addition of S^{2-} in the medium. The decreasing of the potential continued for a specific time depending on the concentration of sulfide ions in the solution: it increases after 5 minutes for the concentration of 10-20 ppm S^{2-} and it stabilizes at -860 mV for 100 ppm. This deviation of E_{corr} is complemented by the formation of non-adhesive black layer of sulfides of copper [28].

To evaluate the inhibitory effect of the chitosan on the evolution of copper potential, we are interesting to realize this study in seawater environment in presence of the chitosan. We can observe that in hopper seawater, the potential shifted towards more negative values and stabilized after 20min of immersion. In other hand, when the chitosan was added, it takes just 5 to 10min to be established at more positive potential values. In fact, this result proves the aptitude of chitosan molecules to protect the copper metal by forming a protective layer on the copper surface. However, when the chitosan was added to synthetic seawater (Figure 3), the decreasing of the copper potential becomes less important.

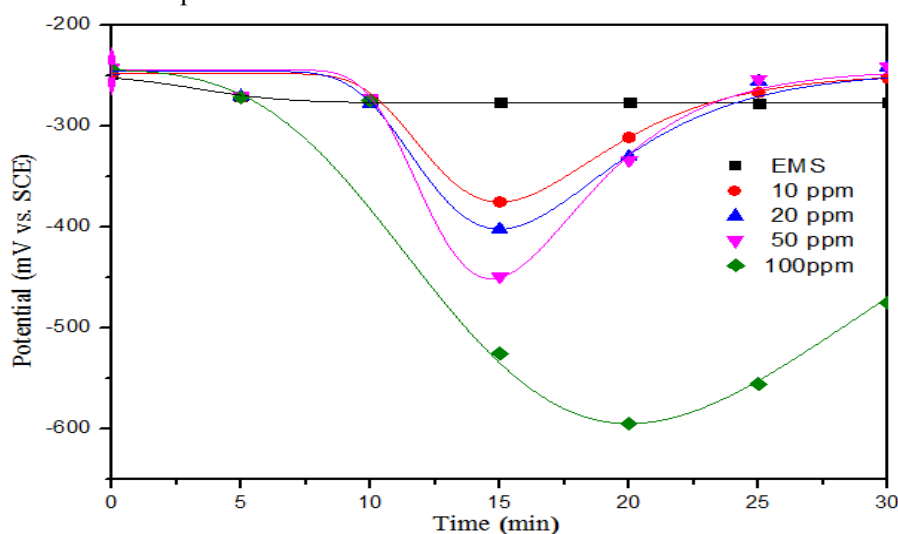


Figure 3: Open circuit potential for the copper immersed in synthetic seawater containing chitosan at different concentration of sulfide ions.

When the sulfide was added at 15min of immersion, the decreasing of the potential was reduced to more positive values compared to seawater in absence of chitosan. For the addition of sulfide at 100ppm, the S^{2-} is not considered as corrosion activator because the potential increases to find the initial value after a definite immersion time.

3.2. Cyclic voltammetry studies

3.2.1. Effect of potential and scan rate on copper behavior

Figure 4 shows the cyclic voltammograms of copper in synthetic seawater with a progressively increasing potential limit in the anodic sweep at a scan rate of 20mV/s.

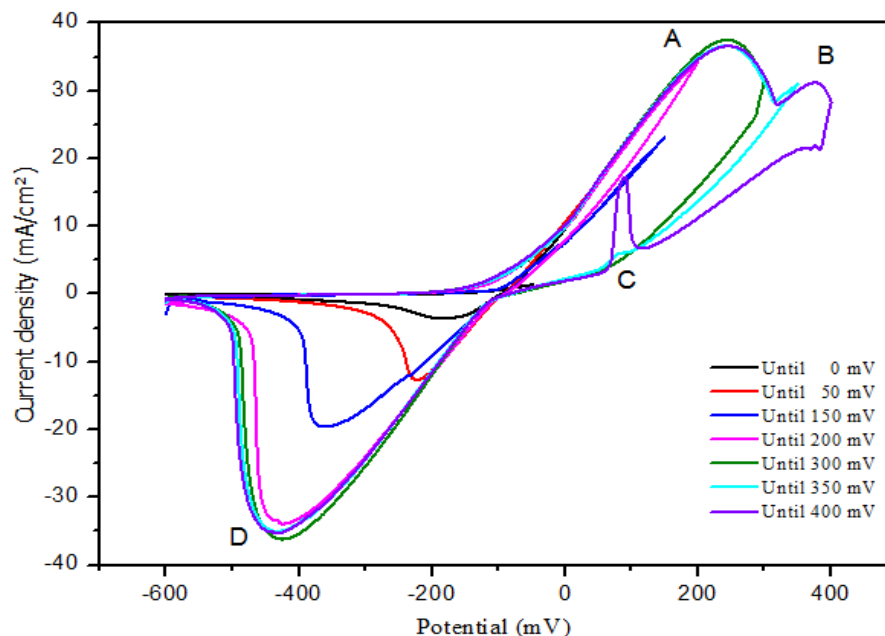
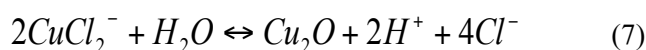
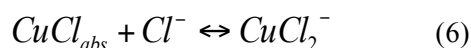


Figure 4: CV for copper in synthetic seawater with a progressively increasing potential limit in the anodic sweep at $V=20\text{mV/s}$

We can attribute the observed difference in the curves, to different reactions of the electrode surface and can be recognized by the anodic and cathodic branches of the voltammograms.

In the anodic curve, the apparition of oxidation peaks depends of the potential limit: when the curve was scanned from -600mV to 0mV , 50mV , 150mV , 200mV , 300mV , we have only one oxidation peak (A) at 242mV due to $\text{Cu}-\text{Cu}^+$ couple. The copper dissolution in synthetic seawater containing chloride starts by the formation of the CuCl which is non-soluble and adsorbed at copper surface. Then, the CuCl is converted to the soluble copper chloride complex CuCl_2^- , if this complex is found in copper surface; it leads to formation of Cu_2O , by [29]:



However, the current density of the peaks varies with the potential domain from 11mA/cm^2 to 37mA/cm^2 . When the potential range exceeded 350mV and 400mV , the second peak (B) appears about 376mV with a current density of $31,21\text{mA/cm}^2$ due to $\text{Cu}^+-\text{Cu}^{2+}$ [30]. In the reverse sweep we obtained only one cathodic peak (C) is observed due to corresponding reduction reaction of copper electrode in synthetic seawater.

In order to evaluate the influence of the scan rate (from 1mV/s to 100mV/s) on the shape of voltammograms of copper immersed in synthetic seawater, we are testing different values of scan rate and the results are examined and regrouped in the Figure 5.

The results indicate that the density current of the both oxidation peaks increased and the potential shifts towards more positive values with increasing of the scan rate. The first scan rate value tested is $V=1\text{mV/s}$, at this rate we observed only one anodic peak. When the scan rate increases, the second oxidation peak appears clearly but it decreases at $V=100\text{mV/s}$. The same profile is respected by the evolution of the current density of the cathodic peak.

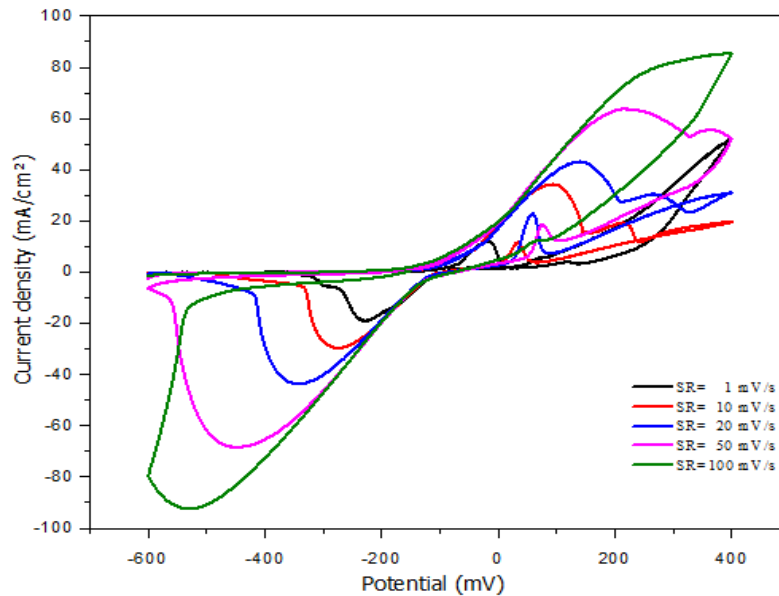


Figure 5: the CV curves of copper in synthetic seawater under different scan rates

Figure 6 presents the dependence of the current density on (scan rate)^{1/2}. A linear correlation is observed which doesn't pass at the origin. This result means that the reactions occurred at the copper dissolution, are partial controlled by diffusion [31].

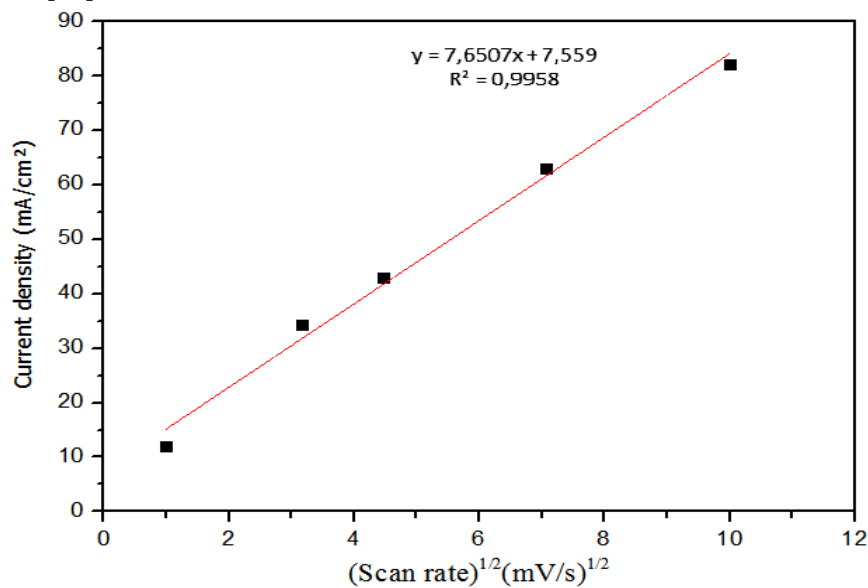


Figure 6: Relation between the current density of first oxidation peak vs. (scan rate)^{1/2} for copper in synthetic seawater in the absence and presence of different concentrations of sulfides at 25 ± 2

3.2.2. Effect of sulfides addition on the copper behavior

The effect of increasing addition of Na₂S concentration on the copper corrosion in synthetic seawater environment has been studied by cyclic voltammetry measurements at a scan rate of 1 mV/s. The figure 7 shows CV curves for copper in seawater in absence and presence of various concentrations of sulfides.

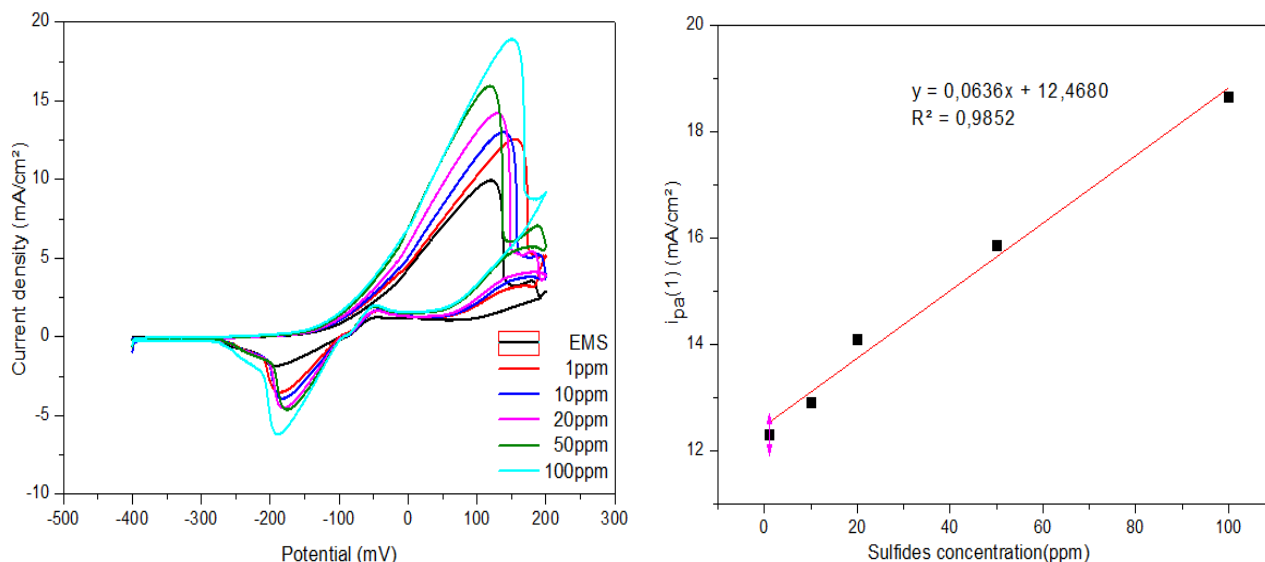
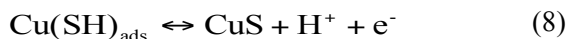


Figure 7: the CV curves of copper and the current density evolution of $i_{pa}(1)$ in synthetic seawater containing different sulfide concentrations at $V=1\text{mV/s}$ in the absence and presence of different concentrations of sulfides at 25 ± 2

Figure 7 shows that both in non-polluted and polluted seawater by sulfides, we have the same CV behavior, but the current density and potential of the anodic and cathodic peaks changes. We observed that the current density is depending on the sulfides concentrations: at 1ppm and 10ppm of sulfides, we have the same behavior registered for non-polluted seawater with increasing in the current density, then the copper-oxide is predominant in both non-polluted and sulfides containing seawater (1ppm and 10ppm) because the copper surface is not completely covered by sulfide ions. The higher current density of first oxidation peak was registered at 100ppm and it increases if the sulfides concentration increases. This increase of current density in presence of sulfides can be justified by the formation of a non-protective copper-sulfide (Cu_2S) layer instead of the protective copper-oxide (Cu_2O) by the catalyzing faculty of the sulfides to prevent oxide-formation and therefore, increase the corrosion attack [30]. At the pH range from 8 to 13, the predominant sulfide species is the hydrosulfide ion (HS^-) [32]. The presence of HS^- in the solution promotes the increase of the copper dissolution simultaneously to the formation of CuS and Cu_2S :



Many studies suggest that the corrosive effect of the sulfides is due to the increase in S^{2-} and HS^- activity in the corrosive solution as the sulfide dissolves. The reason why the sulfide ions are activator ions which accelerates localized and pitting corrosion and made a strong contact adsorption on the surface metal [31]. The copper sulfide resulted catalyzes the anodic reaction (Eq. 8 and 9) [33]. It is excellently demonstrated that the CuS and Cu_2S are corrosion promoters [8, 34].

3.2.3. Effect of chitosan on the copper behavior

The cyclic voltammograms of copper immersed in synthetic seawater in the absence and presence of the chitosan molecules in the potential range -400mV to $+200\text{mV}$ at 1mV/s are exposed in Figure 8. It appears from these plots that the current density decreases to some extent in the anodic curve when the chitosan was added at 1000ppm in the solution. We can suggest that a protective film has been formed on the copper surface in order to inhibit the dissolution of the metal. The CV profiles confirm the chitosan inhibitor functions and protection of Cu from corrosion in a seawater environment. The decrease of the anodic current in solutions in presence of inhibitor is a result of the decreased chloride ion attack on the copper surface due to inhibitor molecule adsorption [35]. We suggest that the addition of chitosan inhibitor decreases the corrosion due to the formation of a protective layer of copper-chitosan complex:



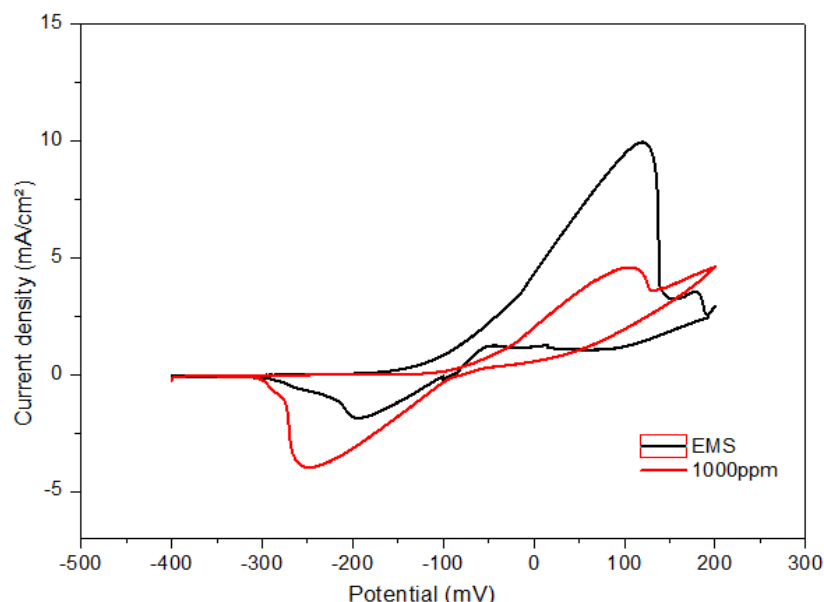


Figure 8: CV of copper in synthetic seawater in the absence and presence of chitosan (1000ppm) at $V=1\text{mV}/\text{min}$

The figure 9 shows the effect of chitosan addition on the CV of copper in synthetic seawater polluted by 20ppm of sulfides at $V=1\text{mV}/\text{s}$.

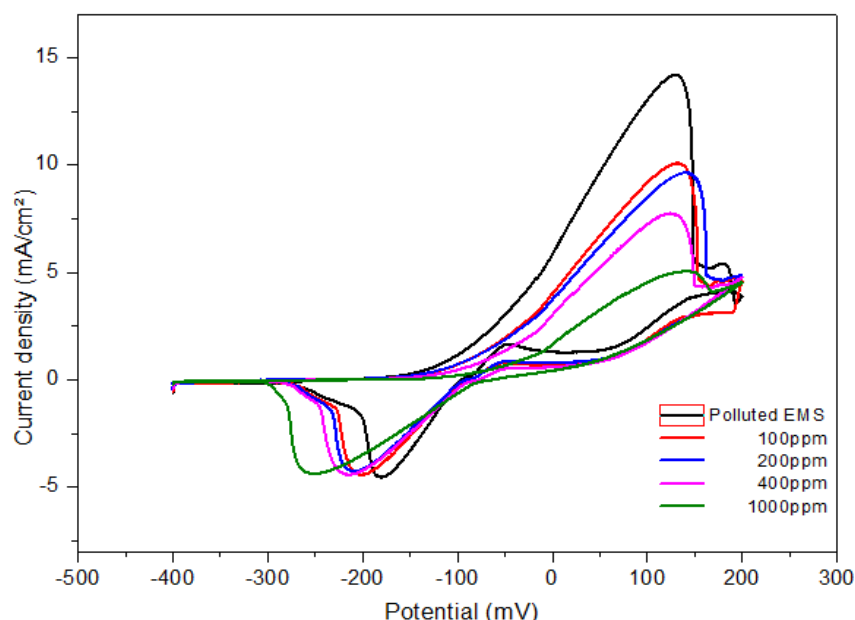


Figure 9: CV of copper in sulfides containing synthetic seawater in the absence and presence of chitosan (2000ppm) at $V=10\text{mV}/\text{min}$

Those voltammograms of copper have an identical shape in different concentrations of the chitosan in the presence of 20ppm of sulfides. We noted that the addition of the chitosan decreased clearly the current density on the first oxidation. This current density increased more with the increasing on the chitosan concentration to reach $5\text{ mA}/\text{cm}^2$ instead of $14.1\text{ mA}/\text{cm}^2$ respectively in the presence (1000ppm) and absence of the chitosan.

The chitosan was found to decrease the copper oxidation in polluted seawater, because of the competitive adsorption between the HS^- ions and chitosan molecules on the copper surface as following [36]:



The important observation is that the evolution of the CV shapes of copper at different concentrations of sulfide in absence of chitosan is comparatively similar to this evolution in presence of chitosan inhibitor. Accordingly the corrosion and corrosion inhibition is related to the sulfides activity in the marine environment. In other hand, we observe that another peak appears at 60 mV. Its current density increases with the increasing of current density of the second oxidation. We attribute it to the reduction of Cu II to Cu I.

3.3. Polarization curves

The Figure 10 presents the results of the effect of sulfides addition on the anodic and cathodic curves of the copper immersed in synthetic seawater at 25 ± 2 . The electrochemical parameters calculated from the polarization curves are given in Table 2. The corrosion rate is calculated as the following:

$$CR(\text{mm/y}) = \frac{(3.268 \times 10^{-3}) \times (i_{\text{corr}} \times M_{\text{Cu}})}{np} \quad (12)$$

Where M_{Cu} refers the copper molecular weight, p is the samples density ($p=8.94 \text{ g/cm}^3$) and n is the electrons number transferred in corrosion reaction.

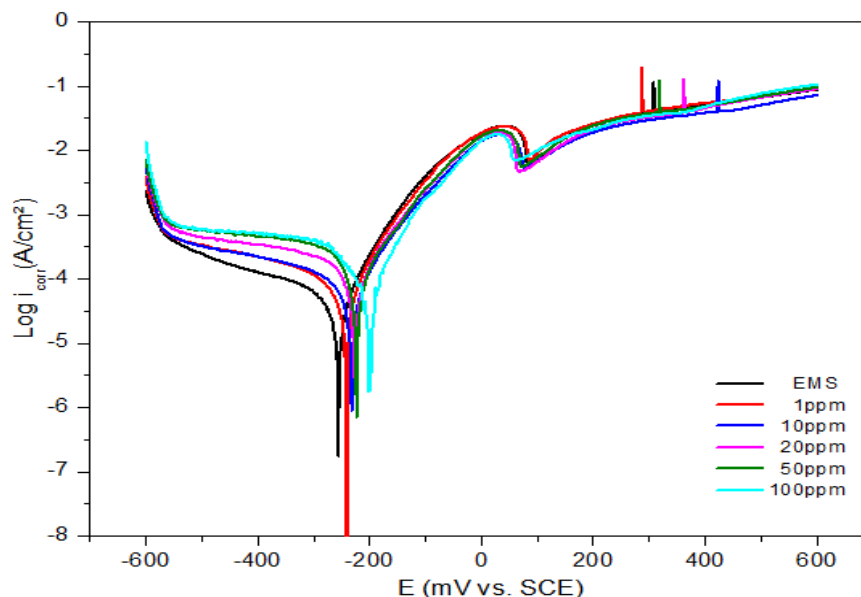


Figure 10: Potentiodynamic polarization curves for copper corrosion in synthetic seawater in the absence and presence of different concentrations of sulfides at 25 ± 2

The results of the sulfides effect revealed the corrosive action of sulfides at the all tested concentrations. It can be seen that 20ppm of sulfides increases the corrosion rate to 1.10 mm/y. Furthermore, when the sulfides concentration increases, the corrosion rate decreased. It is also shown that in the cathodic polarization curve, a diffusion palier was observed when the seawater was polluted with sulfide. In order to clarify and explain this obtained result, we are studying the copper electrochemical

Table 2: Electrochemical parameters obtained from potentiodynamic polarization measurements for copper in sulfide polluted seawater

	E_{corr} (mV)	I_{corr} ($\mu\text{A/cm}^2$)	b_a (mV)	b_c (mV)	R_p (ohm. cm^2)	CR (mm/y)
T	-256.3	39.8	70.5	-306.6	505.76	0.46
1ppm	-243.3	75.6	82.9	-291.8	341.57	0.88
10ppm	-232.9	76.5	91.0	-291.4	320.67	0.89
20ppm	-227.3	94.4	86.0	-164.4	201.45	1.10
50ppm	-224.0	72.2	77.6	-77.5	172.25	0.84
100ppm	-222.9	51.4	107.7	-409.2	216.94	0.60

3.4. Electrochemical impedance tests

The Figure 11 indicates the Nyquist plots of copper in non-polluted seawater and sulfide polluted seawater at various potential values: -260mV, -300mV, -400Mv and -500mV. As can be observed, the Nyquist plots changes depending on the potential values. We can translate this result by the variation of reduction mechanism of the Oxygen. At $E=-260\text{mV}$, we have a charge transfer mechanism in the cathodic curve. But, the impedance measured at -300mV show the the oxygen is reduced at the copper surface by a mixed mechanism. In addition, concerning the more negative potential, we observed a diffusion mechanism with confirms the palier obtained for the oxygen reduction.

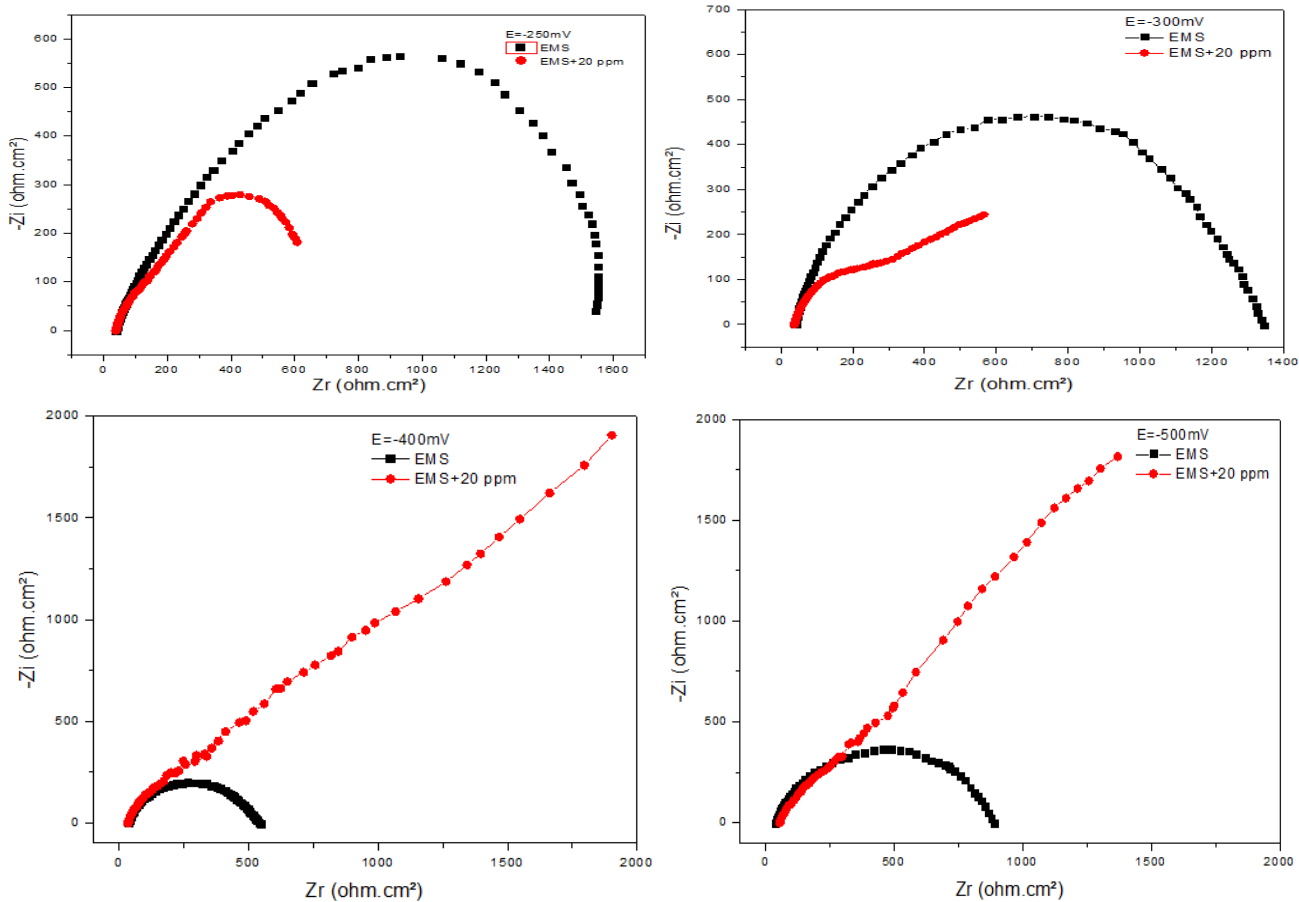


Figure 11: Nyquist presentation for copper immersed non-polluted and sulfide polluted seawater different potential values.

3.2. Surface morphological analysis

The figure 12 shows a comparison between coupon surfaces of copper with sulfide element after three months of immersion in synthetic seawater environment.

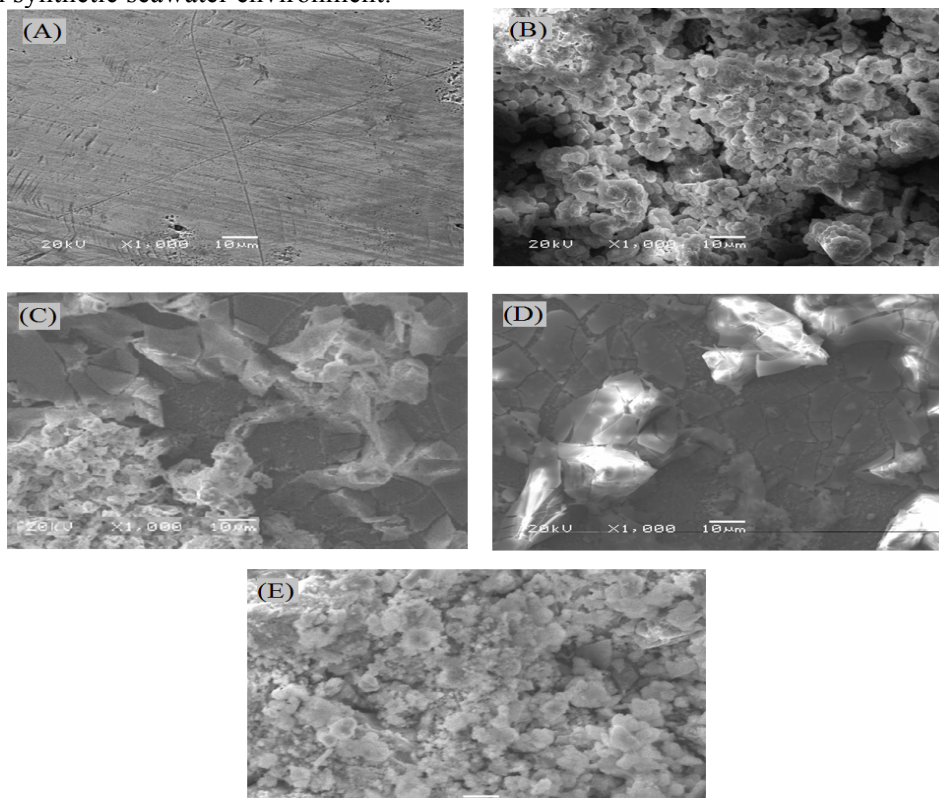


Figure 12: SEM images of copper after three months of exposure to synthetic seawater solution without (A) and with 10ppm (B), 20ppm (C), 50ppm (D) and 100ppm (E) of sulfides

We observe that large amounts of scratches are observed on the copper surface, indicating that the formed corrosion scales on the surface were thin at the addition of 5ppm of sulfides (Figure 12A). However, in the presence of 10ppm of sulfide, only a few scratches are observed due to the thicker corrosion scales covering the surface (Figure 12B). Moreover, we have some irregularly-shaped particles which are distributed on the surface. In the Figure 12C, the copper surface was more homogenous in presence of 20ppm of sulfides because of the formation of copper sulfide in the entire surface. However, the figure 13 designs the EDS graphs for copper immersed for three months in synthetic seawater with and without sulfides. It can be see that the electrode surface contains the chlorine, the Oxygen, the copper and sulfur. This result can prove that the layer formed along the immersion time is constituted by copper oxide and copper sulfide.

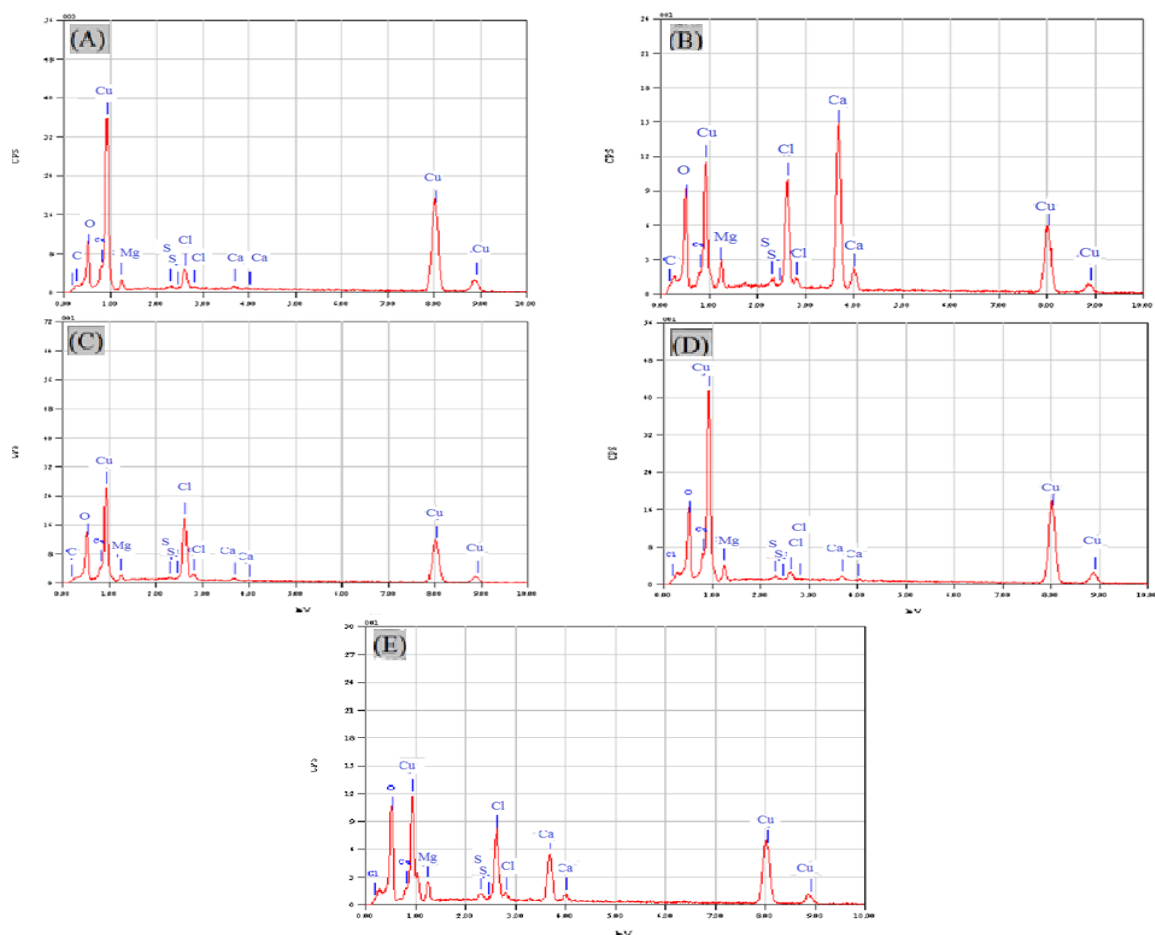


Figure 13: EDS spectra of representative patina samples from: (A) an immersion of copper in EMS without; (B) with 10ppm, 20ppm (C), 50ppm (D) and 100ppm (E) for three months measurements

Conclusion

The present work was carried out in synthetic seawater containing Na_2S with and without chitosan inhibitor using copper electrodes. The two electrochemical methods employed reveal that the addition of sulfide ions in the synthetic seawater environment shifts the potential towards more negative values and increases the current density of copper oxidation, so, the sulfides were demonstrated as the corrosion activator by accelerating the copper oxidation. The scan rate and potential limit variation affect the copper voltammograms shape. The chitosan was investigated as a potential corrosion inhibitor to protect the copper metal against the dissolution in non-polluted and polluted seawater by sulfides by reducing the current density of the oxidation peak. It was found preventing the copper oxidation, especially, at high concentration of the biopolymer.

Acknowledgments- One of the authors (EL MOUADEN Khadija) expresses her gratitude for support from Morocco CNRST (Centre National pour la Recherche Scientifique & Technique) through the excellence scholarship of searching program (2014 Edition).

References

1. L. Smith, B. Nisbet, and E. Wade. 2nd Ed ed, N. 17, *European Federation of Corrosion Publications* 2002.
2. S. Eliassen and L. Smith. 3rd Ed ed, N. 16, *European Federation of Corrosion Publications* 2009.
3. *Deep Repository for Spent Nuclear Fuel* S.T.R. SR-97 Post Closure Safety, Editor, SKB Swedish Nuclear Fuel & Waste Management Co 1999.
4. K. Elmouaden, et al., *Int. J. Electrochem. Sci.* 10 (2015) 7955-7965.
5. K. Pedersen, *Microbial processes in radioactive waste disposal.*, SKB Swedish Nuclear Fuel and Waste Management Co 2000.
6. M. Krufft, et al., *Surf. Sci.* 377 (1997) 601–604.
7. J. Chen, Z. Qin, and D.W. Shoesmith, *J. Electrochem. Soc.* 157 (2010) C338–C345.
8. S. Jacobs and M. Edwards, *Water Res.* 34 (2000) 2798.
9. M.B. McNeil, A.L. Anos, and T.L. Woods., *Corros. Sci.* 49 (1993) 755.
10. A.S. Hamdy, et al., *Int. J. Electrochem. Sci.* 3 (2008) 1142 – 1148.
11. R. Vazquez-Duhalt, et al., *Bioconjugate Chem.* 12 (2001) 301.
12. T. Uragami, et al., *J. Membrane Sci.* 88 (1994) 243.
13. K. Kurita, T. Sannan, and Y. Iwakura, *J. Appl. Polym. Sci.* 23 (1979) 511.
14. K. Ohga, Y. Kuraughi, and H. Yanase, *B. Chem. Soc. Jpn.* 60 (1987) 444.
15. E. Onsoyen and O. Skaugrud, *J. Chem. Technol. Biot.* 49 (1990) 395.
16. F.-C.Wu, R.-L. Tseng, and J. Ruey-Shin, *Ind. Eng. Chem. Res.* 38 (1999) 270.
17. H. Blair and T.-C. Ho, *J. Chem. Technol. Biot.* 31 (1980) 6.
18. K. Kurita, Y. Koyama, and A. Taniguchi, *J. Appl. Polym. Sci.* 31 (1986) 1169.
19. R. Maruca, B. Suder, and J. Wightman, *J. Appl. Polym. Sci.* 27 (1982) 4827.
20. T. Vincent and E. Guibal, *Ind. Eng. Chem. Res.* 40 (2001) 1406.
21. Z. Modrzejewska and W. Kaminski, *Ind. Eng. Chem.* 38 (1999) 4946.
22. T.Asakawa, K. Inoue, and T. Tanaka, *Kagaku Kogaku Ronbun.* 26 (2000) 321.
23. B. Gamblin, J. Stevens, and K. Wilson, *Hyperfine Interact.* 112 (1998) 117.
24. S. Bhatia and N. Ravi, *Biomacromol.* 1 (2000) 413.
25. E. Guibal, C. Milot, and J. Tobin, *Ind. Eng. Chem. Res.* 37 (1998) 1454.
26. I. Jha, L. Iyengar, and A. Prabhakara Rao, *J. Environ. Eng.* 114 (1988) 962-974.
27. J.A. Jennings, et al., *Thin Solid Films.* 596 (2015) 83-86.
28. R. Salghi, et al., *Der Pharma Chemica* 4 (2012) 504-510.
29. A.A. Nazeer, E.A. Ashour, and N.K. Allam, *Mater. Chem. Phys.* 144 (2014) 55-65.
30. B.V. Appa Rao and K. Chaitanya Kumar, *Arab. J. Chem.* 2013.
31. M.A. Deyab and S.T. Keera, *Egyptian J. Petroleum* .21 (2012) 31-36.
32. N.K. Allam, et al., *Corros. Sci.* 47 (2005) 2280-2292.
33. B.V. Appa Rao, K.C.K., *J. Mater. Sci. Technol.* 30 (2014) 65-76.
34. B.C. Syrett, *Corros. Sci.* 21 (1981) 187-209.
35. S. Issaadi, T. Douadi, and S. Chafaa, *Appl. Surf. Sci.* 316 (2014) 582-589.
36. N.K. Allam, H.S. Hegazy, and E.A. Ashour, *Int. J. Electrochem. Sci.* 2 (2007) 549 - 562.

(2017) ; <http://www.jmaterenvirosci.com>